

RESEARCH ARTICLE

Are the severity of obstruction and the apnea–hypopnea index related to orofacial anatomy in children with obstructive sleep apnea? a kinetic MRI study

¹Fabio Savoldi, ²Kevin KF Fung, ³Wing-Sze Mak, ²Elaine YL Kan, ¹Yanqi Yang, ⁴Ka-Li Kwok and ¹Min Gu

¹Orthodontics, Division of Paediatric Dentistry and Orthodontics, Faculty of Dentistry, the University of Hong Kong, Hong Kong, Hong Kong SAR, PRC; ²Department of Radiology, Hong Kong Children's Hospital, Hong Kong, Hong Kong SAR, PRC; ³Department of Diagnostic and Interventional Radiology, Kwong Wah Hospital, Hong Kong, Hong Kong SAR, PRC; ⁴Department of Paediatrics, Kwong Wah Hospital, Hong Kong, Hong Kong SAR, PRC

Objectives: The proportionality between anatomical characteristics and disease severity in children and adolescents with obstructive sleep apnea (OSA) has not been well characterized. The present study investigated the relationship between the dentoskeletal and oropharyngeal features of young patients with OSA and either the apnea–hypopnea index (AHI) or the amount of upper airway obstruction.

Methods: MRI of 25 patients (8- to 18-year-old) with OSA (mean AHI = 4.3 events/h) was retrospectively analyzed. Sleep kinetic MRI (kMRI) was used to assess airway obstruction, and static MRI (sMRI) was used to assess dentoskeletal, soft tissue, and airway parameters. Factors related to AHI and obstruction severity were identified with multiple linear regression (significance level $\alpha = 0.05$).

Results: As evidenced by kMRI, circumferential obstruction was present in 44% of patients, while laterolateral and anteroposterior was present in 28%; as evidenced by sMRI, obstructions were retropalatal in 64% of cases and retroglottal in 36% (no nasopharyngeal obstructions); kMRI showed a higher prevalence of retroglottal obstructions compared to sMRI ($p = 0.037$); the main obstruction airway area was not related to AHI; the maxillary skeletal width was related to AHI ($\beta = -0.512, p = 0.007$) and obstruction severity ($\beta = 0.625, p = 0.002$); and the retropalatal width was related to AHI ($\beta = -0.384, p = 0.024$) and obstruction severity ($\beta = 0.519, p = 0.006$).

Conclusions: In children and adolescents, the severity of OSA and obstruction were inversely proportional to the maxillary basal width and retropalatal airway width. Further studies are needed to assess the benefits of targeted clinical treatments widening the transverse dimension of these structures.

Dentomaxillofacial Radiology (2023) 52, 20220422. doi: [10.1259/dmfr.20220422](https://doi.org/10.1259/dmfr.20220422)

Cite this article as: Savoldi F, Fung KKF, Mak W-S, Kan EYL, Yang Y, Kwok K-L, et al. Are the severity of obstruction and the apnea–hypopnea index related to orofacial anatomy in children with obstructive sleep apnea? a kinetic MRI study. *Dentomaxillofac Radiol* (2023) 52, 20220422.

Keywords: Magnetic Resonance Imaging; Airway Obstruction; Maxilla; Child

Introduction

Background

Pediatric obstructive sleep apnea (OSA) has a multifactorial pathogenesis that may include lymphoid tissue hypertrophy, soft tissue enlargement, and altered craniofacial morphology.^{1–3} Although continuous positive airway pressure reduces mortality, early diagnosis may have a greater impact on disease complications,⁴ and accurate diagnostics are fundamental for targeted clinical treatments.^{2,5} For example, the decision to use a mandibular advancement device, which repositions the tongue anteriorly by moving the lower jaw forward,⁶ or to perform rapid maxillary expansion, which widens the oral cavity by opening the midpalatal suture,⁷ may be based on the type and level of airway obstruction.

MRI is a non-ionizing method that can be safely used in children,⁸ allowing a three-dimensional analysis that overcomes the limitations of two-dimensional X-rays.⁹ In particular, compared to static MRI (sMRI), kinetic MRI (kMRI) provides dynamic assessment owing to more accurate diagnosis for childhood OSA,^{2,10} and it can be performed during induced sleep, which may guide therapy better than awake assessments.¹¹ kMRI also allows quantitative measurements and can be paired with sMRI for evaluating the dual—“soft” and “hard”—anatomical components that contribute to obstruction onset.¹

Reports showing kMRI findings in asleep children with OSA are scarce. One study compared changes in airway shape during tidal breathing between 10 children with OSA and 10 controls.¹² A second study compared kMRI and drug-induced sleep endoscopy (DISE) in identifying airway obstruction in 15 children and adolescents with persistent OSA after adenotonsillectomy.¹³ A third study presented 15 children with Down syndrome and persistent OSA after adenotonsillectomy,⁸ and a final study compared the patterns of dynamic airway motion and adenoid and tonsil size between 16 young patients with OSA and 16 controls.¹⁴ Interestingly, a previous work has observed a “dose–response” relationship between the apnea–hypopnea index (AHI) and some anatomical characteristics of the airway in adolescents,² which deserves further investigation.

Aim and hypothesis

The present study investigated the relationship between anatomical factors and both OSA severity and the degree of dynamic upper airway obstruction during sleep using kMRI in children and adolescents in Hong Kong. The primary hypothesis was that the main obstruction airway area (from sleep kMRI) was positively correlated with the AHI. The secondary hypothesis was that the static anatomical parameters (from sMRI) were correlated either to the AHI or to the main obstruction area (from sleep kMRI).

Methods

Participants

Clinical records of children and adolescents in Hong Kong from the Department of Pediatrics of Kwong Wah Hospital were screened retrospectively. Records of patients up to 18-year-old and with OSA (AHI ≥ 1.0 events/h) who received both sMRI and kMRI for upper airway assessment were further analyzed. Children presenting with craniofacial syndromes, cleft palate, or history of previous surgical or orthodontic treatment of the maxillofacial region were excluded. MRI records showing evident motion artifacts or swallowing action were also excluded, and 25 patients were identified. The sample size was based on the minimum requirement of 25 patients for performing linear regression analysis,¹⁵ with the inclusion of up to six independent variables.¹⁶ The study was approved by the Research Ethics Committee of the Hospital Authority Hong Kong Kowloon Central Cluster and Kowloon East Cluster (KC/KE-20–0318/ER-4).

PSG and MRI acquisition

In-bed overnight polysomnography (PSG) was performed in a pediatric sleep laboratory by a physician specialist in sleep medicine and a polysomnographic technologist. PSG recording and scoring were performed according to the guidelines of the American Academy of Sleep Medicine.

MRI scans were obtained (Achieva XR 1.5 Tesla, Philips Medical Systems, Best, Netherlands) with patients positioned supine with the head in neutral position. The sagittal plane was oriented on the midline. First, a pre-sedation sMRI was obtained with proton density (PD)-weighted turbo spin echo (TSE) images on the sagittal and axial planes (3.0 mm slice thickness, 0.3 mm slice gap, 0.7×0.7 mm voxel size, 10.0 ms time to echo, 4300.0 and 5153.0 ms repetition time, respectively). Second, a pre-sedation kMRI was obtained on the sagittal plane to locate the main obstruction site. Last, a post-sedation kMRI was obtained on the axial plane (at the identified site) to assess the main obstruction. kMRI was obtained with T_1 weighted turbo field echo (TFE) images (single-slice, 10.0 mm thickness, 1.0×1.0 mm voxel size, 1.0 s temporal resolution, 120 scans, 3.7 ms time to echo, 7.6 ms repetition time). Sedation was performed by an anesthesiologist to simulate the sleep condition, after oral administration of melatonin 45 min prior to MRI acquisition (to all patients beside one). Sedation was obtained via intravenous administration of midazolam and fentanyl (to all patients beside one who received only fentanyl and melatonin, and two who received only melatonin).

Measurements

Demographic data (age, sex, weight, and height at the time of PSG) were retrieved from medical records, body

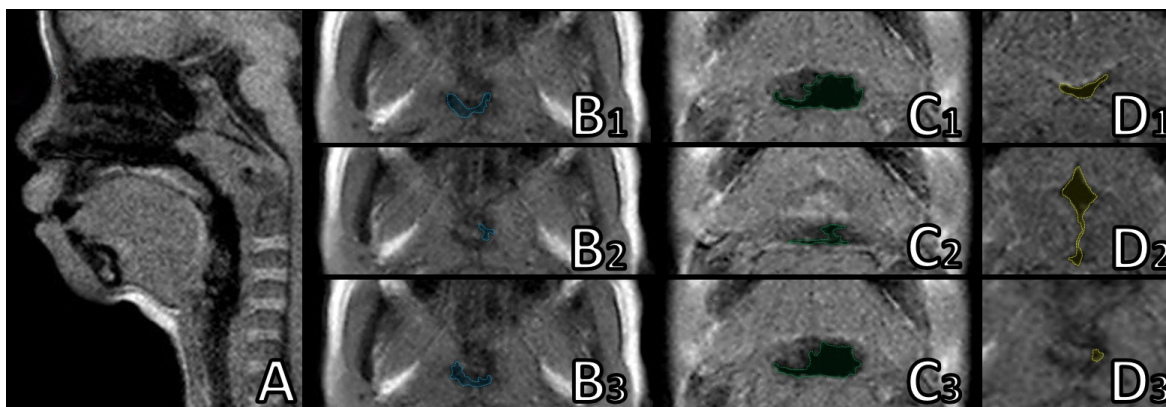


Figure 1 Representative midsagittal kMRI image used for the identification of the main obstruction level (A). Representative serial kMRI images of the retropalatal area (B) and retroglottal area (C), with respective change of the main obstruction area over time (1, airway initially dilated; 2, airway obstructed with minimum area used for measurement; 3, airway finally dilated). Representative axial kMRI images showing anteroposterior (D1), laterolateral (D2), and circumferential (D3) obstruction.

mass index (BMI) was calculated (weight/height),² and AHI was retrieved from PSG records. Skeletal maturity was estimated by using the cervical vertebral maturation (CVM) method.¹⁷ Pre-sedation kMRI on the midsagittal plane was used to assess the main obstruction level (nasopharyngeal, retropalatal, and retroglottal). Post-sedation kMRI on the axial plane (a single 10-mm-thick slice) was used to assess the airway area (defined as the smallest area during airway motion) at the level of the main obstruction, and the obstruction type (anteroposterior, laterolateral, and circumferential) (Figure 1). sMRI was used to assess dentoskeletal, soft tissues, and upper airway morphology, and also to assess

the main obstruction level on the midsagittal plane (Figures 2 and 3). Measurements were taken with dedicated software (Carestream v. 11.1, Carestream Health, Rochester, New York, USA) (Supplementary Figures and Tables).

Bias control, method error and agreement

Records were measured by a radiologist (K.K.F.F., for soft tissues and airway measurements) and by an orthodontist (F.S., for dentoskeletal measurements). Assessors were calibrated on five OSA patients who were excluded from the study. The assessors remeasured all records after a washout period of approximately 1 month. The intra-assessor agreement of continuous variables was calculated with the intraclass correlation coefficient (ICC), and the intra-assessor agreement of categorical variables was calculated with Cohen's *k*-coefficient. The method error was estimated with Dahlberg's formula.¹⁸

Statistical analysis

For continuous variables, the average between the measurements repeated by the same assessor was used. For categorical variables, in case of disagreement between repeated measurements, a further pair of calibrated assessors with similar backgrounds was involved (W.S.M. and M.G., respectively). For continuous variables that were measured on both the left and right sides, the mean was used.

Multiple linear regression models were created setting either the AHI or the area at the main obstruction on the axial plane of sleep kMRI as the outcome variable. The independent variables were dentoskeletal, soft tissue, and airway parameters. For outcome variables, outliers were excluded to avoid undermining the validity of the statistical model.¹⁹ Linearity, homoscedasticity, and normality of the distribution of the residuals were checked. Age, sex, height, CVM, BMI, and axial parapharyngeal fat pads maximum area (PFPA) were used (isolated or in combination) to adjust the

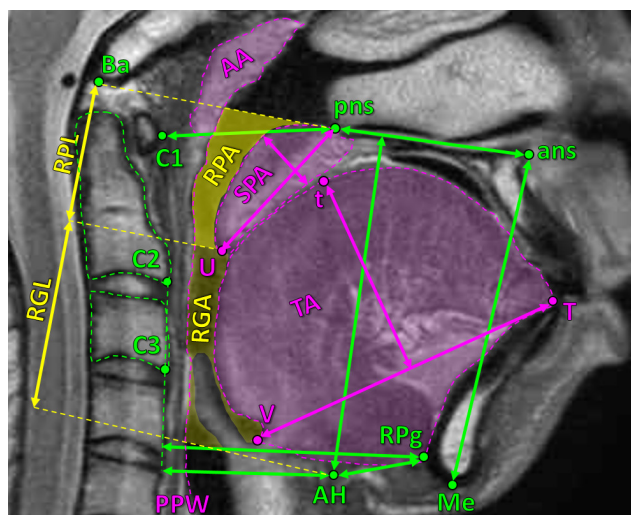


Figure 2 Midsagittal plane analysis on sMRI. Dentoskeletal parameters are reported in green, soft tissue parameters in purple, and upper airway parameters in yellow: anterior nasal spine (ans); posterior nasal spine (pns); first cervical vertebra (C1); second cervical vertebra (C2); third cervical vertebra (C3); anterior hyoid (AH); retroponion (RPg); menton (Me); basion (Ba); vallecula (V); tongue tip (T); superior part of the tongue (t); tongue area (TA); soft palate area (SPA); adenoids area (AA); uvula (U); retropalatal area (RPA); retropalatal length (RPL); retroglottal area (RGA); retroglottal length (RGL).

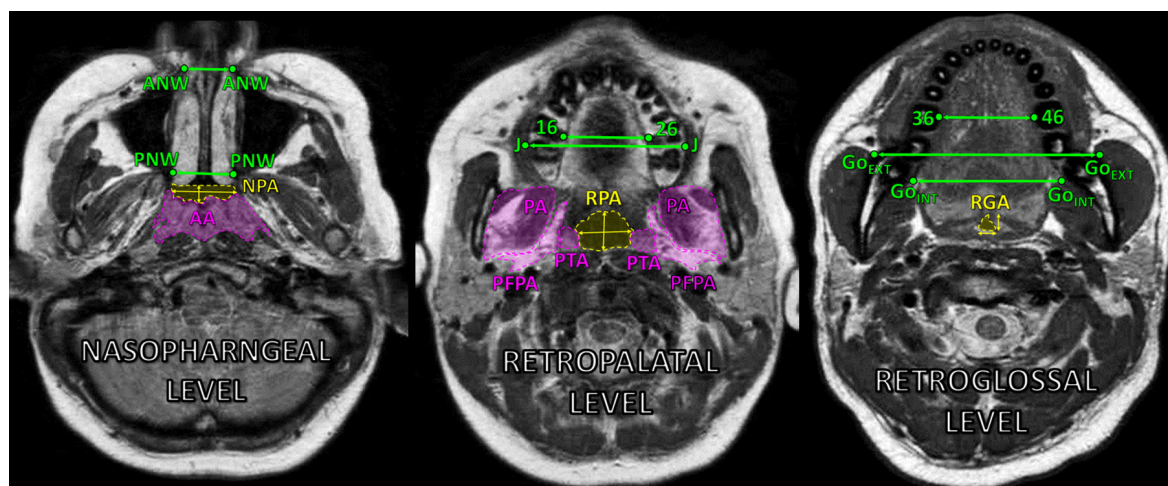


Figure 3 Axial plane analysis at the nasopharyngeal, retropalatal, and retroglossal levels on sMRI. Dentoskeletal parameters are reported in green, soft tissue parameters in purple, and upper airway parameters in yellow: anterior nasal width (ANW); posterior nasal width (PNW); jugal point (J); first upper right molar (16); first upper left molar (26); first lower right molar (36); first lower left molar (46); external mandibular width (Go_{EXT}); internal mandibular width (Go_{INT}); adenoids area (AA); nasopharyngeal area (NPA); retropalatal area (RPA); retroglossal area (RGA). The images do not represent the exact level at which the measurements were taken (as it would have required one image for each parameter): ANW-ANW and PNW-PNW at the most inferior level where the nasal septum is still visible; AA at the level where larger; NPA on the slice closer to posterior nasal spine; 16–26 at the level where the pulp chamber is more visible; J-J at the level of the apex of the upper first molar dental roots; PTA, PA, and PFPA at the level where largest; RPA on the slice where the airway is narrower between posterior nasal spine and uvula; 36–46 at the level where the pulp chamber is more visible; Go_{EXT} - Go_{EXT} and Go_{INT} - Go_{INT} at the level of the apex of the lower first molar dental roots; RGA on the slice where the airway is narrower between uvula and tongue base.

linear regression models. PFPA was used in addition to BMI because it may better represent visceral adiposity in the neck.²⁰ For each parameter, unadjusted and adjusted linear regression models were developed, and those with higher adjusted coefficient of determination (R^2) values were presented. The prevalence of the main obstruction level was compared between presedation kMRI and sMRI with the Pearson χ^2 test. Data were analyzed with statistical software (SPSS v. 23.0, IBM, Armonk, New York, USA) at significance $\alpha = 0.05$.

Results

Method error and agreement

Posterior nasal laterolateral width was excluded from the regression models due to poor intra-assessor agreement (ICC = 0.489). Dentoskeletal measurements showed fair to excellent intra-assessor agreement (ICC from 0.608 to 0.987), similar to soft tissue measurements (ICC from 0.505 to 0.963), and airway measurements showed good to excellent agreement (ICC from 0.741 to 0.965). Obstruction type ($k = 0.761$) and level ($k = 0.754$) on kMRI showed substantial agreement, while obstruction level on sMRI ($k = 0.505$) and CVM staging ($k = 0.516$) showed moderate agreement. The method error was 4.9° for the angular measurement (sagittal soft palate inclination), ranged from 0.6 mm (upper dental arch width) to 4.6 mm (mandibular internal basal width) for linear measurements, and ranged from 7 mm^2 (maximum obstruction airway area) to

140 mm^2 (sagittal tongue area) for the area measurements (Supplementary Table 3).

Descriptive statistics

The sample included 22 males (88%) and 3 females (12%). Patients had a mean age of 13.4 years (SD = 3.1), ranging from 8.1 to 18.4 years, and presented a mean BMI of 20.5 kg/m^2 (SD = 5.1), ranging from 13.3 to 31.7 kg/m^2 . Skeletal maturation assessment showed that 4 patients were at the pre-pubertal skeletal growth stage (CVM 3, 16%), and 21 were at the post-pubertal stage (CVM 4 to 6, 84%). 10 patients received adenotonsillectomy (two patients received lingual frenotomy, two patients received turbinate reduction, and one patient received pharyngoplasty) before MRI and PSG assessment. The mean AHI was 4.3 events/h (SD = 5.9), ranging from 1.0 to 30.1 events/h (Table 1).

The kMRI showed that the main obstruction was retropalatal in 16 cases (64%) and retroglossal in 9 (36%), with no cases of nasopharyngeal obstruction. Of these, 11 obstructions were circumferential (44%), 7 laterolateral (28%), and 7 anteroposterior (28%). The sMRI showed that the main obstruction was retropalatal in 22 cases (88%) and retroglossal in 3 cases (12%), with no case of nasopharyngeal obstruction. A significant difference ($p = 0.037$) was present between pre-sedation kMRI and sMRI in the assessment of the main obstruction level.

Table 1 Descriptive statistics of demographic data and of the variables used for the assessment of sleep, dentoskeletal structures, soft tissues, and airway

	<i>Method</i>	<i>Unit</i>	<i>Mean</i>	<i>SD</i>	<i>Min</i>	<i>Max</i>
Demographic parameters						
Age	Clinical folder	years	13.4	3.1	8.1	18.4
Height	Clinical folder	cm	149.7	18.2	101.3	176.0
Weight	Clinical folder	kg	48.3	19.3	13.8	83.1
BMI	Clinical folder	kg/m ²	20.5	5.1	13.3	31.7
Sleep parameters						
AHI	PSG	events/h	4.3	5.9	1.0	30.1
Dentoskeletal parameters						
Maxillary anteroposterior length	sMRI	mm	50.5	7.9	24.5	61.1
Hyoid superoinferior position	sMRI	mm	58.9	9.5	43.1	75.2
Hyoid anteroposterior position with respect to vertebrae	sMRI	mm	30.7	5.0	21.1	42.0
Hyoid anteroposterior position with respect to chin	sMRI	mm	28.7	5.2	19.1	36.9
Maxillomandibular anteroposterior relationship	sMRI	°	3.5	3.4	-1.5	10.5
Lower anterior facial height	sMRI	mm	67.5	6.9	52.7	79.3
Retromandibular anteroposterior space	sMRI	mm	57.1	7.5	43.9	74.2
Retromaxillary anteroposterior space	sMRI	mm	27.8	4.0	15.8	36.2
Maxillary basal laterolateral width	sMRI	mm	65.6	4.9	55.0	74.5
Anterior nasal laterolateral width	sMRI	mm	21.6	1.9	18.8	26.9
Posterior nasal laterolateral width	sMRI	mm	27.7	3.3	22.1	37.9
Upper dental arch laterolateral width	sMRI	mm	35.1	3.1	27.8	42.6
Mandibular external basal laterolateral width	sMRI	mm	80.9	6.5	65.8	92.7
Mandibular internal basal laterolateral width	sMRI	mm	41.6	6.6	28.5	56.8
Lower dental arch laterolateral width	sMRI	mm	36.1	3.3	29.6	42.4
Soft tissue parameters						
Sagittal adenoids area	sMRI	mm ²	216.5	79.6	103.6	412.3
Sagittal tongue area	sMRI	cm ²	24.6	5.7	12.8	37.0
Sagittal tongue length	sMRI	mm	67.8	8.9	47.3	83.3
Sagittal tongue thickness	sMRI	mm	38.1	4.7	28.5	47.3
Sagittal soft palate area	sMRI	mm ²	271.4	57.1	161.9	352.6
Sagittal soft palate length	sMRI	mm	30.1	4.0	22.1	38.4
Sagittal soft palate inclination	sMRI	°	124.3	8.5	108.7	137.8
Sagittal soft palate thickness	sMRI	mm	9.9	1.0	7.5	11.6
Axial palatal tonsils maximum area	sMRI	mm ²	174.2	72.6	12.1	315.1
Axial parapharyngeal fat pads maximum area	sMRI	mm ²	88.2	36.0	31.9	168.2
Axial pterygoid muscle maximum area	sMRI	mm ²	302.0	79.6	192.5	500.2
Axial adenoids maximum area	sMRI	mm ²	420.9	89.9	233.1	597.5
Airway parameters						
Main obstruction airway area	kMRI	mm ²	45.7	34.2	1.3	139.9
Sagittal retropalatal area	sMRI	mm ²	198.4	57.5	29.5	298.8
Sagittal retropalatal craniocaudal length	sMRI	mm	25.4	4.6	15.2	35.7
Sagittal retroglossal area	sMRI	mm ²	362.9	109.8	162.0	541.1
Sagittal retroglossal craniocaudal length	sMRI	mm	34.3	5.9	20.8	46.4
Axial nasopharyngeal airway area	sMRI	mm ²	201.8	108.1	30.7	430.1
Axial nasopharyngeal maximum anteroposterior diameter	sMRI	mm	11.8	5.4	4.3	22.8
Axial nasopharyngeal maximum laterolateral diameter	sMRI	mm	21.4	5.0	9.7	29.9
Axial retropalatal airway area	sMRI	mm ²	51.9	38.7	12.4	166.5
Axial retropalatal maximum anteroposterior diameter	sMRI	mm	5.9	2.7	2.0	13.3
Axial retropalatal maximum laterolateral diameter	sMRI	mm	10.8	4.1	4.9	19.4
Axial retroglossal airway area	sMRI	mm ²	95.8	45.3	23.7	193.4
Axial retroglossal maximum anteroposterior diameter	sMRI	mm	10.5	4.2	4.6	22.0
Axial retroglossal maximum laterolateral diameter	sMRI	mm	12.4	4.4	3.3	20.1

AHI = apnea-hypopnea index; BMI = body mass index; Max = maximum; Min = minimum; PSG = polysomnography; SD = standard deviation; kMRI = kinetic magnetic resonance imaging; sMRI = static magnetic resonance imaging.

Linear regression models

Diagnostics of the linear regression models were performed (Supplementary Material 1). The main obstruction airway area was not related to the AHI.

Maxillary basal laterolateral width ($\beta = -0.498$, $p = 0.013$), sagittal soft palate length ($\beta = -0.433$, $p = 0.035$), axial nasopharyngeal ($\beta = -0.559$, $p = 0.004$) and retropalatal ($\beta = -0.407$, $p = 0.048$) maximum laterolateral width were inversely correlated with the AHI (Table 2). However, by adjusting for sex, age, height, BMI, CVM, and PFPA, only maxillary basal laterolateral width ($\beta = -0.573$, $p = 0.008$) and axial retropalatal maximum laterolateral width ($\beta = -0.408$, $p = 0.040$) were still correlated with AHI (Figure 4, Table 2).

Maxillary basal laterolateral width ($\beta = 0.414$, $p = 0.040$), axial retropalatal airway area ($\beta = 0.415$, $p = 0.039$), and axial nasopharyngeal ($\beta = 0.466$, $p = 0.019$) and retropalatal ($\beta = 0.536$, $p = 0.006$) maximum laterolateral width were directly correlated to the main obstruction area on kMRI, while sagittal tongue length ($\beta = -0.426$, $p = 0.034$) was inversely related to it (Table 3). However, by adjusting for sex, age, height, BMI, CVM, and PFPA, only the maxillary basal laterolateral width ($\beta = 0.633$, $p = 0.011$), axial retropalatal airway area ($\beta = 0.507$, $p = 0.024$), axial nasopharyngeal maximum laterolateral width ($\beta = 0.649$, $p = 0.004$) and axial retropalatal maximum laterolateral width ($\beta = 0.515$, $p = 0.016$) were still correlated with the main obstruction area on kMRI (Table 2 and Figure 4).

Discussion

Relationship between obstruction and severity of OSA

The present study aimed to identify factors related to the severity of the disease in patients with OSA and not to explain its etiopathogenesis compared to healthy individuals, since this would require a control group. Perhaps surprisingly, the main obstruction area of the airway that was assessed with kMRI during induced sleep was not correlated to the AHI. It is possible that the proportionality between these variables was not linear, compromising the ability of the linear model to detect it.²¹ However, it is also possible that no proportionality existed between OSA severity and amount of dynamic airway obstruction during sleep in this group of patients, which is in agreement with a previous study comparing PSG findings with static airway assessment in awake patients.²²

Relationship between anatomical structures and severity of OSA

Anatomical factors measured in awake patients showed some relationship with the severity of OSA. The first is the width of the retropalatal airway, which findings agree with a previous controlled study showing that the laterolateral dimension of the airway, especially at the retropalatal level, is among the most relevant factors for the onset of OSA.²³ It is worth noting that 40% of the patients included in the present study received

Table 2 Parameters that were significant in at least one of the adjusted models of the linear regression analysis with AHI as primary outcome are shown

	Linear regression models												
	Unadjusted			Adjusted for height and BMI			Adjusted for height, BMI and CVM			Adjusted for all factors ^a			
	β	p-value	R ²	β	p-value	R ²	β	p-value	R ²	β	p-value	R ²	
AHI vs airway parameters on kMRI													
Main obstruction airway area	NR	NS	NR	NR	NS	NR	NR	NS	NR	NR	NS	NR	NR
AHI vs dentoskeletal parameters on sMRI													
Maxillary basal laterolateral width	-0.498	0.013	0.213	-0.456	0.012	0.479	-0.512	0.007	0.494	-0.573	0.008	0.439	0.439
AHI vs soft tissue parameters on sMRI													
Sagittal soft palate length	-0.433	0.035	0.150	NR	NS	NR	NR	NS	NR	NR	NS	NR	NR
AHI vs airway parameters on sMRI													
Axial nasopharyngeal maximum laterolateral width	-0.559	0.004	0.282	NR	NS	NR	NR	NS	NR	NR	NS	NR	NR
Axial retropalatal maximum laterolateral width	-0.407	0.048	0.128	-0.384	0.024	0.446	-0.381	0.028	0.420	-0.408	0.040	0.327	0.327

AHI = apnea-hypopnea index; BMI = body mass index; CVM = cervical vertebral maturation; NR = not reported; NS = not significant; kMRI, kinetic magnetic resonance imaging; sMRI, static magnetic resonance imaging; β , standardized regression coefficient.
R² = adjusted coefficient of determination.
The model with the highest adjusted R² is reported in bold.
The unadjusted model, the models adjusted for the most relevant factors, and the full model are reported for each significant parameter.
^a Height, BMI, CVM, age, sex and paralaryngeal fat pads area.

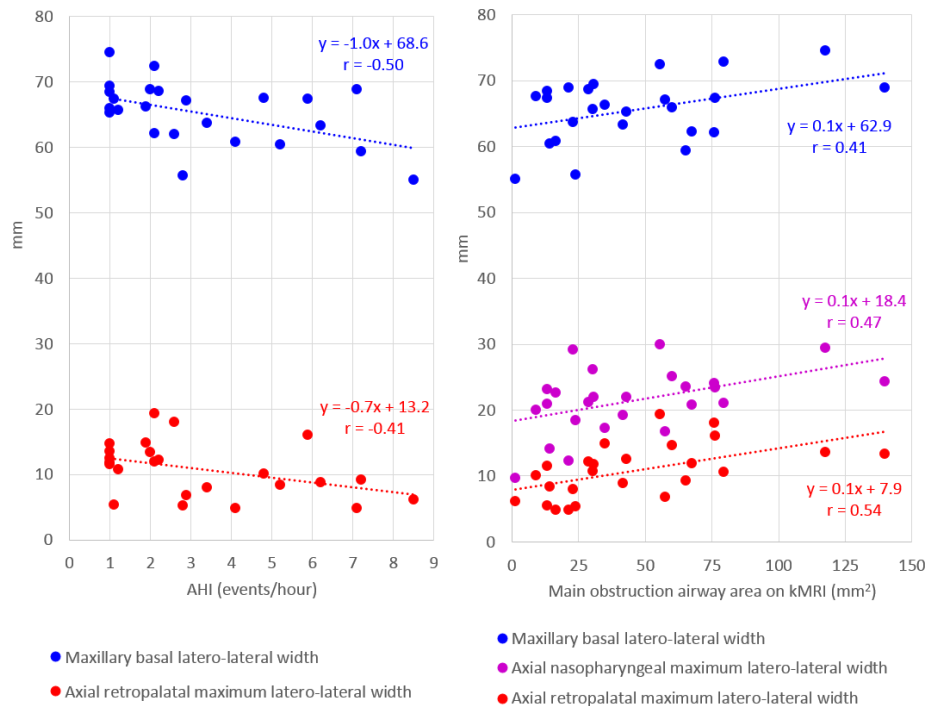


Figure 4 Scatter plots and trend lines representing the most relevant parameters (significant in all models of the linear regression analysis). Bivariate correlations between the AHI and static anatomical parameters (**left**) and between the main obstruction airway area on kMRI and static anatomical parameters (**right**) are reported. Regression equations and Pearson's correlation coefficients (r) are reported for each regression line. AHI, apnea-hypopnea index; kMRI, kinetic MRI

adenotonsillectomy, which may explain the low prevalence of obstructions at the nasopharyngeal level but may also bias the relevance of these structures in the presented analysis. In fact, a previous study in obese adolescents showed a significant correlation between adenoid and tonsil volume and AHI,² and the contribution of lymphoid tissue to OSA severity reported in the present study should be interpreted with caution. The second factor is the width of the maxillary basal bone. Although previous studies showed no differences in maxillary width between children with OSA and controls,¹⁻³ measurements were based on the dental structure, which did not appear to be significant in the present work as well. In fact, a meta-analysis reported a reduction in the AHI following skeletal maxillary expansion,²⁴ and the present study may be the first report showing a negative correlation between the skeletal width of the maxillary basal bone and the AHI.

Relationship between anatomical structures and severity of obstruction

Defining the presence of obstruction may be more challenging than fixing an AHI value for diagnosing OSA. The mean obstruction area on kMRI during induced sleep was 45mm², and it is uncertain whether such values may correspond to clinically relevant obstructions. A previous study using sMRI showed a mean minimum oropharyngeal cross-sectional area of 50mm² in 4- to 15-year-old children with OSA,¹ which is compatible with the present

findings. According to another study using kMRI,¹² no complete airway obstruction was noticed, except for one patient with an almost complete obstruction (1.3mm²). Nevertheless, it is also possible that induced sleep may not replicate natural sleep well, or that the duration of the kMRI acquisition was not long enough to allow obstruction to happen (as a mean of 4.3 obstructive events were present every hour). The basal laterolateral width of the maxilla was correlated with the amount of obstruction during induced sleep. Direct proportionality was present, meaning that the larger the skeletal base of the maxilla was, the larger the airway area was (*i.e.* the less severe the obstruction was). Accordingly, widening of the skeletal base of the maxilla has been associated with enlargement of the airway in children with OSA.²² Even though the present findings may be interpreted such that the larger the expansion is, the greater the reduction of the obstruction, biological limits should be carefully considered because of possible adverse effects related to excessive maxillary expansion.^{25,26} This said, sleep kMRI showed that almost half of the patients had circumferential collapse, while the remaining patients were equally distributed between latero-lateral collapse and antero-posterior collapse. Unfortunately, the sample size did not allow a subanalysis based on the obstruction type, and further studies are advisable for understanding the effect of phenotypic subtyping on the importance of maxillary skeletal width.²⁷ The relevance of the laterolateral component was further supported by the fact that retropalatal

Table 3 Parameters that were significant in at least one of the adjusted models of the linear regression analysis with main obstruction area on kMRI as primary outcome are shown

Linear regression models												
	Unadjusted			Adjusted for height			Adjusted for height and PFFA			Adjusted for all factors ^a		
	β	R ²	p-value	β	R ²	p-value	β	R ²	p-value	β	R ²	p-value
Main obstruction area on kMRI vs dentoskeletal parameters on sMRI												
Maxillary basal laterolateral width	0.414	0.135	0.040	0.625	0.002	0.367	0.601	0.004	0.345	0.633	0.011	0.253
Main obstruction area on kMRI vs soft tissue parameters on sMRI												
Sagittal tongue length	-0.426	0.034	0.034	NR	NS	NS	NR	NS	NR	NR	NS	NR
Main obstruction area on kMRI vs airway parameters on sMRI												
Axial nasopharyngeal maximum laterolateral width	0.466	0.183	0.019	0.623	0.001	0.386	0.643	0.001	0.442	0.649	0.004	0.333
Axial retropalatal airway area	0.415	0.136	0.039	0.409	0.037	0.188	NR	NS	NR	0.507	0.024	0.187
Axial retropalatal maximum laterolateral width	0.536	0.256	0.006	0.511	0.007	0.287	0.519	0.006	0.323	0.515	0.016	0.221

NR = not reported; NS = not significant; PFFA = parathyroid gland fat pads; kMRI = kinetic magnetic resonance imaging; sMRI, static magnetic resonance imaging; β , standardized regression coefficient.

R² = adjusted coefficient of determination.

The model with the highest adjusted R² is reported in bold.

The unadjusted model, the models adjusted for the most relevant factors, and the full model are reported for each significant parameter.

^a Height, PFFA, cervical vertebral maturation, age, sex and body mass index.

^b β = standardized regression coefficient.

and retroglossal maximum laterolateral widths were the most significant predictors of obstruction severity among the airway measurements. In fact, the thickness of the muscles of the lateral pharyngeal walls may have a critical role in apneic patients.²³

Comparison between static and kinetic MRI

A significant reduction in the prevalence of retropalatal collapse, together with a respective increase in the prevalence of retroglossal collapse, was noticed from static to kinetic MRI. In fact, OSA is a dynamic phenomenon, and static imaging alone may not be suitable for its analysis.²⁸ Changes in the main obstruction level might also be expected after sedation, as sleep influences the dynamics of OSA.¹¹ However, in the present study, the level of collapse was identified on the sagittal plane of pre-sedation kMRI, and post-sedation kinetic imaging was performed on the axial plane of this identified level. Thus, any change in the main level of obstruction from pre- to post-sedation may have reduced the validity of the presented assessment.

Limitations

The prevalence of males was approximately seven times higher than the prevalence of females. Accordingly, sleep-disordered breathing has a higher prevalence in males.²⁹ In particular, the vast majority of patients included in the present study were at post-pubertal skeletal growth, and sex-related differences are more likely to emerge after puberty.³⁰ In addition, despite the anesthesiologist aimed at achieving a level of sedation that was similar to deep sleep, it is possible that the sedation level was not equal among patients. Although limiting the analysis to Chinese children from Hong Kong has addressed the reported need to include more ethnically diverse populations in this area of research,²⁷ it may also have limited the applicability of these findings to other populations. Prospective kMRI studies in asleep children, preferably with stratified sampling based on OSA severity and obstruction type, are advisable to clarify the clinical outcomes of orthodontic and surgical treatments affecting maxillary and the retropalatal airway anatomy.

Conclusions

Within the limitations of the present study and related to non-syndromic children and adolescents from Hong Kong with OSA, the MRI assessment showed that:

- A greater width of the maxillary basal bone was proportional to less severe OSA and to less severe upper airway obstruction during induced sleep.
- Static measurement of the nasopharyngeal and retropalatal laterolateral width of the airway in awake patients were the most significant predictors of the severity of both OSA and airway obstruction during induced sleep.

- Differences were present between static and dynamic airway assessments regarding the level of collapse in awake patients, and complementary dynamic assessment might be advisable for better diagnosis and treatment planning.

Acknowledgements

The authors wish to thank Ms. Shuk-Yu Leung (Department of Paediatrics, Kwong Wah Hospital, Hong Kong S.A.R.) for contributing to the data collection, and Ms. Samantha K.Y. Li (Faculty of Dentistry, the University of Hong Kong, Hong Kong S.A.R.) for contributing to the data analysis. The present work was part of the thesis for the Master of Dental Surgery in Orthodontics of Dr. Fabio Savoldi (Dental School, University of Brescia, Italy).

Contributors

Conception and design: F.S., K.K.F.F., W.S.M., and E.Y.L.K.; data acquisition: F.S., K.K.F.F., W.S.M., and M.G.; data analysis and preparation of figures and tables: F.S.; data interpretation: F.S., K.K.F.F., and M.G.; drafting of the manuscript: F.S.; critical revision: K.K.F.F., W.S.M., M.G., Y.Y., E.Y.L.K. and K.L.K. All authors approved the final version submitted for publication.

Funding

This study was partially supported by the Health and Medical Research Fund (Research GrantNumber: 06171176) of the Research Fund Secretariat (Food and Health Bureau, Hong KongS.A.R.).

Data Availability

The data that supports the findings of this study are available in the supplementary material of this article.

Ethics approval

The study was approved by the Research Ethics Committee of the Hospital Authority Hong Kong Kowloon Central Cluster and Kowloon East Cluster (KC/KE-20-0318/ER-4).

Disclosure

Authors declare no conflict of interest.

REFERENCES

- Cappabianca S, Iaselli F, Negro A, Basile A, Reginelli A, Grassi R, et al. Magnetic resonance imaging in the evaluation of anatomical risk factors for pediatric obstructive sleep apnoea-hypopnoea: a pilot study. *Int J Pediatr Otorhinolaryngol* 2013; **77**: 69–75. <https://doi.org/10.1016/j.ijporl.2012.09.035>
- Schwab RJ, Marcus CL, all of the study authors. Reply: understanding the anatomic basis for obstructive sleep apnea syndrome in adolescents: how to proceed? *Am J Respir Crit Care Med* 2015; **192**: 1295–1309. <https://doi.org/10.1164/rccm.201507-1292LE>
- Arens R, McDonough JM, Costarino AT, Mahboubi S, Tayag-kier CE, Maislin G, et al. Magnetic resonance imaging of the upper airway structure of children with obstructive sleep apnea syndrome. *Am J Respir Crit Care Med* 2001; **164**: 698–703. <https://doi.org/10.1164/ajrccm.164.4.2101127>
- Jennum P, Kjellberg J. Health, social and economical consequences of sleep-disordered breathing: a controlled national study. *Thorax* 2011; **66**: 560–66. <https://doi.org/10.1136/thx.2010.143958>
- Op de Beeck S, Dieltjens M, Verbruggen AE, Vroegop AV, Wouters K, Hamans E, et al. Phenotypic labelling using drug-induced sleep endoscopy improves patient selection for mandibular advancement device outcome: a prospective study. *Journal of Clinical Sleep Medicine* 2019; **15**: 1089–99. <https://doi.org/10.5664/jcs.7796>
- Gu M, Savoldi F, Chan EYL, Tse CS, Lau MT, Wey MC et al. Changes in the upper airway, hyoid bone, and craniofacial morphology between patients treated with headgear activator and Herbst appliance: a retrospective study on lateral cephalometry. *Orthod Craniofac Res* 2020; **24**: 360–9.
- Savoldi F, Wong KK, Yeung AWK, Tsoi JKH, Gu M, Bornstein MM. Midpalatal suture maturation staging using cone beam computed tomography in patients aged between 9 to 21 years. *Sci Rep* 2022; **12**: 4318.
- Shott SR, Donnelly LF. Cine magnetic resonance imaging: evaluation of persistent airway obstruction after tonsil and adenoidectomy in children with Down syndrome. *The Laryngoscope* 2004; **114**: 1724–29. <https://doi.org/10.1097/00005537-200410000-00009>
- Savoldi F, Xinyue G, McGrath CP, Yang Y, Chow SC, Tsoi JK et al. Reliability of lateral cephalometric radiographs in the assessment of the upper airway in children: A retrospective study. *Angle Orthod* 2020; **90**: 47–55.
- Liu SY, Huon LK, Lo MT, Chang YC, Capasso R, Chen YJ et al. Static craniofacial measurements and dynamic airway collapse patterns associated with severe obstructive sleep apnoea: a sleep MRI study. *Clin Otolaryngol* 2016; **41**: 700–6.
- Fishman G, Zemel M, DeRowe A, Sadot E, Sivan Y, Koltai PJ. Fiber-optic sleep endoscopy in children with persistent obstructive sleep apnea: inter-observer correlation and comparison with awake endoscopy. *Int J Pediatr Otorhinolaryngol* 2013; **77**: 752–5.
- Arens R, Sin S, McDonough JM, Palmer JM, Dominguez T, Meyer H, et al. Changes in upper airway size during tidal breathing in children with obstructive sleep apnea syndrome. *Am J Respir Crit Care Med* 2005; **171**: 1298–1304. <https://doi.org/10.1164/rccm.200411-1597OC>
- Clark C, Ulualp SO. Multimodality assessment of upper airway obstruction in children with persistent obstructive sleep apnea after adenotonsillectomy. *Laryngoscope* 2017; **127**: 1224–30.
- Donnelly LF, Surdulescu V, Chini BA, Casper KA, Poe SA, Amin RS. Upper airway motion depicted at cine MR imaging performed during sleep: comparison between young Patients with and those without obstructive sleep apnea. *Radiology* 2003; **227**: 239–45.
- Jenkins DG, Quintana-Ascencio PF. A solution to minimum sample size for regressions. *PLoS One* 2020; **15**: e0229345.
- Austin PC, Steyerberg EW. The number of subjects per variable required in linear regression analyses. *J Clin Epidemiol* 2015; **68**: 627–36. <https://doi.org/10.1016/j.jclinepi.2014.12.014>
- Baccetti T, Franchi L, McNamara JA. The cervical vertebral maturation (CVM) method for the assessment of optimal treatment timing in dentofacial orthopedics. *Seminars in Orthodontics* 2005; **11**: 119–29. <https://doi.org/10.1053/j.sodo.2005.04.005>
- Dahlberg G. *Statistical Methods for Medical and Biological Students*. London: George Allen and Unwin; 1940.
- Stevens JP. Outliers and influential data points in regression analysis. *Psychological Bulletin* 1984; **95**: 334–44. <https://doi.org/10.1037/0033-2909.95.2.334>
- Schwab RJ, Pasirstein M, Pierson R, Mackley A, Hachadoorian R, Arens R, et al. Identification of upper airway anatomic risk factors for obstructive sleep apnea with volumetric magnetic resonance imaging. *Am J Respir Crit Care Med* 2003; **168**: 522–30. <https://doi.org/10.1164/rccm.200208-866OC>
- Leatherbarrow RJ. Using linear and non-linear regression to fit biochemical data. *Trends Biochem Sci* 1990; **15**: 455–58. [https://doi.org/10.1016/0968-0004\(90\)90295-m](https://doi.org/10.1016/0968-0004(90)90295-m)
- Caprioglio A, Meneghel M, Fastuca R, Zecca PA, Nucera R, Nosetti L. Rapid maxillary expansion in growing patients: correspondence between 3-dimensional airway changes and polysomnography. *Int J Pediatr Otorhinolaryngol* 2014; **78**: 23–27. <https://doi.org/10.1016/j.ijporl.2013.10.011>
- Schwab RJ, Gupta KB, Geftter WB, Metzger LJ, Hoffman EA, Pack AI. Upper airway and soft tissue anatomy in normal subjects and patients with sleep-disordered breathing: significance of the lateral pharyngeal walls. *Am J Respir Crit Care Med* 1995; **152**: 1673–89. <https://doi.org/10.1164/ajrccm.152.5.7582313>
- Huynh NT, Desplats E, Almeida FR. Orthodontics treatments for managing obstructive sleep apnea syndrome in children: a systematic review and meta-analysis. *Sleep Med Rev* 2016; **25**: 84–94. <https://doi.org/10.1016/j.smrv.2015.02.002>
- Brunetto M, Andriani J da SP, Ribeiro GLU, Locks A, Correa M, Correa LR. Three-Dimensional assessment of buccal alveolar bone after rapid and slow maxillary expansion: a clinical trial study. *Am J Orthod Dentofacial Orthop* 2013; **143**: 633–44. <https://doi.org/10.1016/j.ajodo.2012.12.008>
- Garib DG, Henriques JFC, Janson G, de Freitas MR, Fernandes AY. Periodontal effects of rapid maxillary expansion with tooth-tissue-borne and tooth-borne expanders: a computed tomography evaluation. *American Journal of Orthodontics and Dentofacial Orthopedics* 2006; **129**: 749–58. <https://doi.org/10.1016/j.ajodo.2006.02.021>
- Zinchuk A, Yaggi HK. Phenotypic subtypes of OSA: a challenge and opportunity for precision medicine. *Chest* 2020; **157**: 403–20. <https://doi.org/10.1016/j.chest.2019.09.002>
- Donnelly LF, Shott SR, LaRose CR, Chini BA, Amin RS. Causes of persistent obstructive sleep apnea despite previous tonsillectomy and adenoidectomy in children with Down syndrome as depicted on static and dynamic cine MRI. *American Journal of Roentgenology* 2004; **183**: 175–81. <https://doi.org/10.2214/ajr.183.1.1830175>
- Lumeng JC, Chervin RD. Epidemiology of pediatric obstructive sleep apnea. *Proc Am Thorac Soc* 2008; **5**: 242–52. <https://doi.org/10.1513/pats.200708-135MG>
- Ersu R, Arman AR, Save D, Karadag B, Karakoc F, Berkem M, et al. Prevalence of snoring and symptoms of sleep-disordered breathing in primary school children in Istanbul. *Chest* 2004; **126**: 19–24. <https://doi.org/10.1378/chest.126.1.19>